

d-wave Charge-4*e* Superconductivity From Fluctuating Pair Density Waves

Yi-Ming Wu¹ and Yuxuan Wang^{2,*}

¹*Stanford Institute for Theoretical Physics, Stanford University, Stanford, California 94305, USA*

²*Department of Physics, University of Florida, Gainesville, Florida 32611, USA*

(Dated: August 13, 2024)

We present a theory for charge-4*e* superconductivity as a leading low-temperature instability with a nontrivial *d*-wave symmetry. We show that in several microscopic models for the pair-density-wave (PDW) state, when the PDW wave vectors connect special parts of the Fermi surface, the predominant interaction is in the bosonic pairing channel mediated by exchanging low-energy fermions. This bosonic pairing interaction is repulsive in the *s*-wave channel but attractive in the *d*-wave one, leading to a *d*-wave charge-4*e* superconductor. By analyzing the Ginzburg-Landau free energy including higher-order fluctuation effects of PDW, we find that the charge-4*e* superconductivity emerges as a vestigial order of PDW, and sets in via a first-order transition. Both the gap amplitude and the transition temperature decay monotonically with increasing superfluid stiffness of the PDW order. Our work provides a microscopic mechanism of higher-charge condensates with unconventional ordering symmetry in strongly-correlated materials.

Introduction.— Charge-4*e* superconductivity (4*e*-SC) is an exotic order in which four fermions are bound together and condense [1–6], with a nonvanishing order parameter $\sim \langle \psi_i \psi_j \psi_k \psi_l \rangle$ (where ψ_j is some fermion field with a proper quantum number j). Compared with the more common charge-2*e* superconductivity (2*e*-SC) whose order parameter is $\sim \langle \psi_i \psi_j \rangle$, it breaks the global $U(1)$ symmetry to a discrete \mathbb{Z}_4 symmetry, in a sense that the discrete global gauge transformation $\psi_j \rightarrow \psi_j e^{in\pi/2}$ ($n = 1, 2, 3, 4$) leaves the order parameter invariant. The fact that a 4*e*-SC state is from binding four fermions can be reflected by the Little-Parks experiment, which was used as a direct proof of Cooper pairing phenomenon in 2*e*-SC state. A recent such study was carried out on the Kagome metal CsV₃Sb₅ [7], where a charge-4*e* signal was observed in the normal state. However, whether one can observe the charge-4*e* bounding in the superconducting state remains an active ongoing research topic. On the theory side, recent progress has been made in understanding the properties of a 4*e*-SC [8, 9], which is in general an nontrivial interacting system even at the mean-field level (unlike the Bogoliubov-de Gennes Hamiltonian of a 2*e*-SC in which fermionic excitations are free). It was found [8] that 4*e*-SC has a superfluid density perturbative in the order parameter, and is in general a gapless system.

However, the mechanism for 4*e*-SC from interacting fermions remains a theoretical challenge. Unlike 2*e*-SC which follows from an arbitrarily weak attractive interaction, there lacks a logarithmic divergence for the “quadrupling” susceptibility for 4*e*-SC. Some early speculations of inducing 4*e*-SC by disorder [10] or condensing skyrmions in a quadratic band touching system [11] exist. In recent years, a promising framework for understanding 4*e*-SC has emerged from the perspective of intertwined orders [12], in which a plethora of orders breaking distinct symmetries can naturally emerge

from the partial melting of certain primary electronic orders [13–20]. The starting point of such analyses is typically a Ginzburg-Landau (GL) theory for the primary orders, and when the underlying fermionic models are taken into full account, the intrinsic leading instability toward 4*e*-SC are in general subleading to those toward non-superconducting states, either nematic or ferromagnetic [18, 21–23]. It remains a major theoretical challenge to search for microscopic mechanisms for 4*e*-SC as a *leading* instability. Furthermore, in fermionic systems with repulsive interaction, 2*e*-SC orders can emerge with unconventional pairing symmetries; while the pairing symmetry of 4*e*-SC order has been largely unexplored [20, 22] (see also Ref. [24] for an example in cold atom systems).

In this work, we directly demonstrate that in a range of two-dimensional (2d) fermionic models with pair density wave (PDW) instabilities [25–32], a 4*e*-SC order naturally emerges as the leading instability once fluctuation effects are taken into account. Extending the PDW flavor number to large- M which justifies the mean field treatment of the 4*e*-SC order, we establish the GL theory for the 4*e*-SC state by incorporating higher order of interactions for the primary fluctuating PDW fields. (Of course, for $M = 1$, the phase transition in 2d is of Kosterlitz-Thouless nature, and the mean-field transition represents a crossover above the actual transition, but the transition is still driven by precisely the same attractive interaction we identify in this work.) From this effective GL free energy we can determine the nature of 4*e*-SC transition. We find the resulting 4*e*-SC order has a *d*-wave symmetry, and the phase transition from high temperature normal state to 4*e*-SC state is first-order. The transition occurs at $T_c > T_{\text{PDW}}$, where T_{PDW} is the mean-field onset temperature of the primary PDW order. An important quantity that determines T_c is the stiffness κ of the PDW fluctuations, and we find that smaller stiffness yields a higher T_c as well as a larger gap amplitude $|\Delta_{4e}|$, as a larger κ tends to suppress fluctuation effects and is hence detrimental for the development of composite orders. This may shed some new light on finding suitable

* yuxuan.wang@ufl.edu

platform materials for realizing the exotic $4e$ -SC state.

Model and methods. — The starting point of our theory, the PDW state, is by itself an exotic type of superconductivity with Cooper pairs carrying non-zero momenta. We emphasize that a microscopic mechanism for a PDW ground state in connection with realistic materials is not a settled issue. However, in recent years it has been intensely studied and shown to emerge via various microscopic mechanisms [33–53] to emerge. Regardless of the mechanism for PDW, the instability toward $4e$ -SC can be understood as the pairing instability due to interactions among PDW bosons. While in unconventional $2e$ -SC the effective interaction among fermions stems from exchanging bosons, here the effective interactions among bosons result from exchanging fermions, e.g., as illustrated in Fig. 1(a). To make this effective interactions significant, the four fermions in Fig.1(a) need to be as close to the Fermi surface as possible, and this can be realized by invoking a simple geometric relation in a C_4 symmetric system.

In general, these PDW fluctuations can lead to different vestigial orders including CDW, nematic, and $4e$ -SC that are of comparable strength (see, e.g., Refs [18, 22]). However, we will show below that in a C_4 symmetric system, as long as the PDW momentum \mathbf{Q} satisfies

$$\frac{|\mathbf{Q}|}{\sqrt{2}} = |\mathbf{k}_F \bmod (\pi, 0)|, \quad (1)$$

$4e$ -SC order is naturally favored energetically over nematic and CDW orders. Here \mathbf{k}_F corresponds to one of the Fermi surface (FS) portions that are connected by the PDW order parameters, i.e., the PDW hotspots.

Notably, there are several microscopic theoretical models for PDW in which Eq. (1) is satisfied. For example, in Ref. [49], PDW order was shown to emerge from finite-range pair-hopping interactions, either in the continuum [illustrated in Fig. 1(b)] or on a square lattice [Fig. 1(c)]. In Refs. [42, 44], PDW orders develop due to antiferromagnetic exchange interactions in the spin-fermion model proposed for the underdoped cuprates. While the applicability of these microscopic models to real materials remains an open issue, the ubiquity of the relation (1) implies a generic formalism for $4e$ -SC.

Further, we stress that no fine-tuning is needed — we will see that even if Eq. (1) is approximately satisfied, our results will hold. In the continuum, all possible values of \mathbf{Q} form a ring [49], and the ratio Q/k_F can be continuously varied. Moreover, we show in the Supplementary Note I [54] that in several lattice models, this condition is *automatically* satisfied for various values of \mathbf{k}_F and \mathbf{Q} that changes with doping. Below we show that when Eq.(1) is satisfied, the particular interaction in Fig. 1(a) among PDW bosons with momenta $\pm\mathbf{Q}$ and $\pm\mathbf{P}$ (wavevectors related by $\pi/2$ rotations) is parametrically enhanced.

The pairing interaction for PDW bosons are repulsive. We find that the repulsive interaction can lead to bosonic pairing ($4e$ -SC) with unconventional d -wave sym-

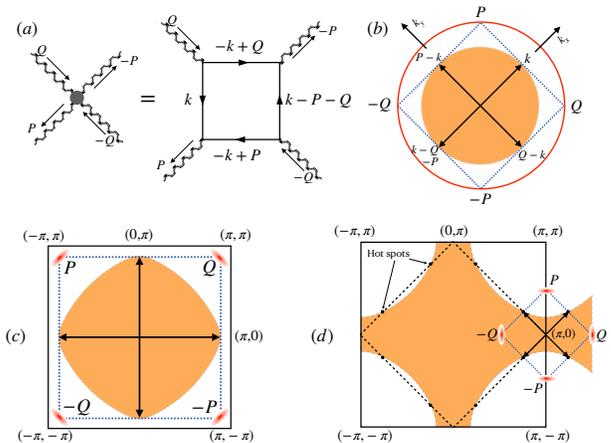


FIG. 1. $4e$ -SC from fluctuating PDW. (a) The effective pairing interaction for PDW bosons via exchanging fermions. Here $\pm\mathbf{Q}$ and $\pm\mathbf{P}$ are related by consecutive $\pi/2$ rotations. When Eq. (1) is satisfied, the internal fermions are on the Fermi surface. (b) Continuum model for PDW with $O(2)$ symmetry from Ref. [49]. The orange area is the filled Fermi sea, and the PDW momentum \mathbf{Q} takes values on the Bose surface represented by the red circle. The model can be continuously tuned such that $|\mathbf{Q}| = \sqrt{2}k_F$. (c) The PDW model realized on a square lattice when the fermions relevant for pairing are close to the Van Hove points $(0, \pi)$ and $(\pi, 0)$ and the PDW momentum is close to (π, π) . (d) PDW fluctuations in the spin-fermion model [42, 44]. The four hot spots (black dots) near $(\pi, 0)$ form a square, and the momenta for the potential PDW orders also form a square. The models in (c) and (d) satisfy the condition in Eq. (1).

metry. We note that this is reminiscent of the situation in fermionic pairing in unconventional superconductors. We develop a mean-field theory to capture the phase transition into the $4e$ -SC phase. To that end, we introduced additional fields corresponding to bosonic bilinears, including the $4e$ -SC order parameter, along with several Lagrange multiplier fields. After integrating out the auxiliary fields, we obtain a free energy for $4e$ -SC, and find that the phase transition is of first order.

Attractive interaction from fluctuating PDW. — As a starting point, we consider a model for fluctuating PDW order with a C_4 symmetry. The analysis for the case with continuous rotation symmetry will be qualitatively similar. Denoting the bosonic PDW field by $\Psi_i(\mathbf{q})$, where \mathbf{q} is measured from the ordering momentum $\mathbf{Q}_i \in \{\pm\mathbf{P}, \pm\mathbf{Q}\}$, the generic free energy up to quadratic order for PDW fluctuations of those examples depicted in Fig. 1 can be written as

$$F = \sum_{i=1}^4 \int \frac{d^2\mathbf{q}}{4\pi^2} [\alpha(T) + \kappa\mathbf{q}^2] |\Psi_i(\mathbf{q})|^2 + \mathcal{O}(\Psi^4) \quad (2)$$

where κ is the amplitude stiffness for the PDW orders obtained by expanding the particle-particle susceptibility to $\mathcal{O}(\mathbf{q}^2)$, and below the mean-field (4) below, this hierarchy allows the $4e$ interaction to be dominant over other

channels. In general, the dispersion of the PDW bosons is anisotropic in \mathbf{q} , but as can be directly checked, for $4e$ -SC instabilities the anisotropy factor can be absorbed into a redefinition of q_x and q_y around each PDW ordering momenta (see the Supplementary Note III [54]). For PDW fluctuations intrinsically driven by finite-range electronic interactions, κ comes from both the particle-particle bubble and from the \mathbf{q} dependence of the interaction, and for weak interactions we assume that $1/\kappa \ll E_F$. Further, as will be explained later, for analytical control of the theory, we are interested in the regime $1/\kappa \ll T_{\text{PDW}} \ll E_F$. This corresponds to a regime in which PDW and $4e$ -SC develop at low energies, and the phase fluctuations of PDW are not “too strong”; see discussions around Eq. (4) and Eq. (10) below. Indeed, in the microscopic theory of Ref. [49], κT_{PDW} can be freely tuned by the interaction strength. Hereafter we measure all lengths against $n^{-1/2}$, where n is electron density, and all energies against the Fermi energy, which, is defined as $E_F \equiv v_F \sqrt{n}$.

The effective interaction between the PDW bosons starts at the order of $|\Psi|^4$. It can be viewed as arising from exchanging fermionic degrees of freedom [see Fig.1(a)]. As is usually done for itinerant fermions, the processes involved are described by square diagrams. The key insight here is that, for dominant four-boson interactions, the internal fermions need to come from the vicinity of the FSs. For systems satisfying Eq.(1), this consideration alone singles out three types of interactions

$$\beta_1 |\Psi_0|^4 + \beta_2 |\Psi_{\pm P}|^2 |\Psi_{\pm Q}|^2 + \beta (\Psi_P \Psi_{-P} \Psi_Q^* \Psi_{-Q}^* + h.c.), \quad (3)$$

where we have used the shorthands, e.g., $|\Psi_0|^4 \equiv \sum_i \int_{\mathbf{q}_1, \mathbf{q}_2, \mathbf{q}_3} \Psi_i(\mathbf{q}_1) \Psi_i^*(\mathbf{q}_2) \Psi_i(\mathbf{q}_3) \Psi_i^*(\mathbf{q}_1 - \mathbf{q}_2 + \mathbf{q}_3)$, and $\int_{\mathbf{q}} \equiv \int \frac{d^2 \mathbf{q}}{4\pi^2}$. Importantly, the last interaction with coefficient β , depicted diagrammatically in Fig. 1(a), is of appreciable strength only when the condition Eq. (1) is satisfied; otherwise at least two fermion propagators would come from regions far away from the FS. The coefficients $\beta_{1,2}$ and β can be readily obtained by integrating out low-energy fermions, and by linearizing the fermionic dispersion we obtain (see Ref. [55] and also the Supplementary Note II [54] for details)

$$\beta_1 \sim 1, \beta_2 \sim \ln \frac{1}{T}, \text{ and } \beta = \frac{1}{16T}. \quad (4)$$

Observe that parametrically, $\beta \gg \beta_{1,2}$ as long as $T \ll 1$ (in original units, $T \ll E_F$). Due to the large separation between β and $\beta_{1,2}$, we expect that even if Eq. (1) hold approximately, one can safely neglect $\beta_{1,2}$.

The last term in Eq. (3) represents a repulsion for the bosons corresponding to PDW fluctuations. As is familiar from $2e$ -SC, repulsive interactions may have attractive components in pairing channels with higher-angular momenta. To this end, we introduce bilinear operators Φ_s and Φ_d for $4e$ -SC with s -wave and d -wave components

$$\Phi_{s/d}(\mathbf{q}) \equiv \int_{\mathbf{p}} \Psi_Q(\mathbf{p} + \mathbf{q}) \Psi_{-Q}(-\mathbf{p}) \pm \Psi_P(\mathbf{p} + \mathbf{q}) \Psi_{-P}(-\mathbf{p}) \quad (5)$$

such that the β interaction can be rewritten as

$$\frac{\beta}{2} \int \frac{d^2 \mathbf{q}}{4\pi^2} |\Phi_s(\mathbf{q})|^2 - \frac{\beta}{2} \int \frac{d^2 \mathbf{q}}{4\pi^2} |\Phi_d(\mathbf{q})|^2. \quad (6)$$

Just like their $2e$ -SC counterparts, $\Phi_{s,d}$ are distinguished by their transformation properties under the C_4 rotation: Φ_s is even and Φ_d is odd. From this decomposition it is evident that in d -wave channel the charge- $4e$ pairing interaction is attractive.

Let us comment on other couplings and fluctuations in other channels. The β_1 term corresponds to a local repulsive interaction between the PDW bosons. The β_2 term is repulsive, but it can be written as $\beta_2 (|\Psi_P|^2 + |\Psi_Q|^2)^2 / 4 - \beta_2 (|\Psi_P|^2 - |\Psi_Q|^2)^2 / 4$, revealing its tendency toward a nematic instability with the order parameter $\mathcal{N} \sim |\Psi_P|^2 - |\Psi_Q|^2$. In several recent works [18, 22] based on two uniform superconducting orders, it was generally found that the vestigial nematic order is more favorable. However, our microscopic calculation has shown that in our PDW-based model, thanks to the C_4 symmetry and the condition in Eq.(1), $4e$ -SC is favored energetically, as $\beta \gg \beta_2$.

We also note that the decomposition of the β -term interaction is not unique. Notably, it can also be decomposed such that there is an equally attractive interaction for a charge-density-wave (CDW) composite order, with e.g., $\rho_{P-Q} = \Psi_P \Psi_Q^* - \Psi_{-Q} \Psi_{-P}^*$. The interplay between CDW and $4e$ -SC has been systematically studied in a phenomenological model [15]. However, in our microscopic model the CDW instabilities are secondary to that of $4e$ -SC. Qualitatively, the reason is similar to the situation in a fermionic theory — in 2d and higher dimensions with weakly-coupled fermions, the CDW instability requires nesting of the FS, that is, fermionic dispersions at different momenta with a fixed difference need to be the same, while the $2e$ -SC instability does not. [55] Here the same reasoning holds for interacting bosons, where the bosonic dispersion for Ψ_P and Ψ_Q is clearly not nested, which can be directly seen from Fig. 1. Therefore, the CDW is suppressed compared with the d -wave $4e$ -SC, even if attractive interactions for these channels are equal (see the Supplementary Note V [54] for a quantitative analysis).

Just like the quartic interactions, higher-order interactions come microscopically from higher-order processes of exchanging low-energy fermions. Making use of the condition in Eq. (1), again only a subset of diagrams need to be included. We present all the dominant interactions at sixth and eighth order in the Supplementary Note II [54], and find that the sixth-order coupling constant γ and eighth-order coupling constant are given by $\gamma = 1/(768T^3)$, and $\zeta = 1/(7680T^5)$.

Formation of d -wave $4e$ -SC.— We obtain a phase transition into a d -wave $4e$ -SC, conspired by fluctuations of the PDW bosons described by Eq. (2), and the attractive interaction in Eq. (6). Formally, the mean-field theory can be justified by extending $\Phi_i(\mathbf{q})$ to an M -component field $\Phi_i^J(\mathbf{q})$ where $J \in [1, M]$ [54–56].

We first take the mean-field ansatz $\mathcal{N} = \Phi_s = 0$. We then have up to eighth order in Ψ (see details in the Supplementary Note III and IV [54])

$$\begin{aligned}
F = & \sum_i \int_{\mathbf{q}} [\alpha(T) + \kappa \mathbf{q}^2] |\Psi_i(\mathbf{q})|^2 - \frac{\beta}{2} \int_{\mathbf{q}} |\Phi_d(\mathbf{q})|^2 \\
& - \frac{\gamma}{4} \int_{\mathbf{q}, \mathbf{p}} \Phi_d(\mathbf{q}) \Phi_d^*(\mathbf{q} + \mathbf{p}) \phi(\mathbf{p}) \\
& + \frac{\zeta}{16} \int_{\mathbf{q}, \mathbf{k}, \mathbf{p}} \Phi_d(\mathbf{q}) \Phi_d^*(\mathbf{q} + \mathbf{p}) \Phi_d(\mathbf{k}) \Phi_d^*(\mathbf{k} - \mathbf{p}) \\
& - \frac{\zeta}{16} \int_{\mathbf{q}, \mathbf{k}, \mathbf{p}} \Phi_d(\mathbf{q}) \Phi_d^*(\mathbf{q} + \mathbf{p}) \phi(\mathbf{k}) \phi^*(\mathbf{k} - \mathbf{p}) + \mathcal{O}(\Psi^{10}),
\end{aligned} \quad (7)$$

where $\phi \equiv |\Psi_{\mathbf{P}}|^2 + |\Psi_{-\mathbf{P}}|^2 + |\Psi_{\mathbf{Q}}|^2 + |\Psi_{-\mathbf{Q}}|^2$ is the Gaussian fluctuation.

The decoupling of the interaction terms of Ψ at any order can be achieved by introducing *two* sets of ancillary fields λ_d, μ and Δ_d, φ , where λ_d and μ are Lagrange multiplier fields ensuring $\Delta_d = \Phi_d$ and $\varphi = \phi$. [54] We can then replace the bilinear operators ϕ and Φ_d with local fields. For quartic interactions we show in the Supplementary Note VI [54] that the result is the same as that from the HS transformation. As a mean-field ansatz, we consider spatially uniform saddle-point solutions, with $\Delta_d(\mathbf{q}) = \Delta_d \delta(\mathbf{q})$, and $\varphi(\mathbf{q}) = \varphi \delta(\mathbf{q})$. Using the regularization $\delta(\mathbf{q} = 0) = V$ where V is the volume (area) of the system and defining the free energy density $\mathcal{F} \equiv F/V$, we have

$$\begin{aligned}
\mathcal{F}[\Psi, \Delta_d, \varphi, \lambda_d, \mu] = & \sum_{i, \mathbf{q}} [r + \kappa \mathbf{q}^2] |\Psi_i(\mathbf{q})|^2 \\
& - \frac{\beta}{2} |\Delta_d|^2 + \frac{\zeta}{16} |\Delta_d|^4 - \frac{\zeta}{16} |\Delta_d|^2 \varphi^2 \\
& + \lambda_d (\Delta_d^* - \Phi_d^*) + \lambda_d^* (\Delta_d - \Phi_d) + \mu \varphi + \mathcal{O}(\Psi^{10}),
\end{aligned} \quad (8)$$

where $r = \alpha(T) - \frac{\gamma}{4} |\Delta_d|^2 - \mu$, $\lambda_d \equiv \lambda_d(\mathbf{q} = 0)/V$, $\mu \equiv \mu(\mathbf{q} = 0)/V$, and we have used the fact that $V \int_{\mathbf{q}} \equiv \sum_{\mathbf{q}}$ in the continuum limit. We note that $\mathcal{F}[\Psi, \Delta_d, \varphi, \lambda_d, \mu]$ is at most quadratic in the field $\Psi(\mathbf{q})$.

Assuming $r > 0$, we can integrate out the PDW fields and get a free energy density $\mathcal{F}(\Delta_d, \varphi, \lambda_d, \mu)$. Generalizing to large- M and taking the saddle points for φ, λ_d, μ , we get up to constant terms

$$\mathcal{F}(\Delta_d)/M = A(T) |\Delta_d|^2 + B(T) |\Delta_d|^4 + C(T) |\Delta_d|^6 + \dots, \quad (9)$$

where the GL coefficients $A(T), B(T)$ and $C(T)$ are determined by the microscopic parameters $\kappa, \alpha, \beta, \gamma$ and ζ and their full expressions are listed in the Supplementary Note IV [54]. One important feature of these coefficients is each of them contains terms that are organized in increasing powers of $1/\kappa T \ll 1$ or $1/\kappa \alpha$. Assuming $\kappa \alpha \gtrsim 1$ as we will justify below, the coefficients can be greatly simplified by keeping the leading contributions,

$$\begin{aligned}
A(T) & \approx \frac{2\pi\alpha\kappa}{T} - \frac{\beta}{2}, \quad B(T) \approx -\frac{4\pi^3\alpha\kappa^3}{3T^3}, \\
C(T) & \approx \frac{64\pi^5\alpha\kappa^5}{45T^5}
\end{aligned} \quad (10)$$

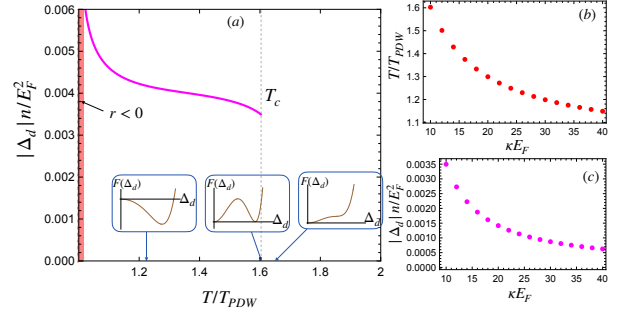


FIG. 2. Phase transition of the leading d -wave $4e$ -SC. (a) $4e$ -SC gap amplitude as a function of T obtained for $T_{\text{PDW}} = 0.1$ and $\kappa = 10$. Inset: GL free energy as a function of Δ_d . (b) and (c) The impact of κ on T_c and Δ_d .

Driven by the temperature dependence of $\alpha(T)$, the quadratic coefficient $A(T)$ becomes negative upon lowering temperature when $\alpha\kappa = \beta T/4\pi \approx 0.005$. At this point, we see that $B(T) < 0$, i.e., $\Delta_d = 0$ is no longer a local minimum of the free energy. Instead, the global minimum of free energy is given by $\Delta_d \neq 0$. Therefore, a first-order phase transition must have already occurred at a higher temperature. The transition temperature is thus set by

$$\alpha_c \sim 1/\kappa, \quad T_c > T_{\text{PDW}}, \quad (11)$$

which can be directly confirmed by minimizing (9) up to sixth order. We see that a smaller stiffness term κ leads to a higher T_c .

Complementary to the analytical approach when $\kappa T \gg 1$, we also solved numerically for saddle points using the full expressions for $A(T), B(T)$, and $C(T)$ in the Supplementary Note IV [54], as is shown in Fig. 2. We see that $|\Delta_d|$ increases monotonically as T decreases below T_c . Once $|\Delta_d|$ becomes large enough, r in Eq. (8) will eventually become negative, invalidating our perturbative analysis. In practice, in the region of $r < 0$ one needs to keep expanding to higher orders of the PDW order parameters. We also show the free energy profile for $T > T_c, T = T_c$ and $T < T_c$, from which the nature of first order phase transition is seen directly. In order to show the impact of the stiffness κ on various quantities for the $4e$ -SC order, we show in Fig. 2(b) and (c) the plot of T_c and $|\Delta_d(T_c)|$ as a function of κ . It is clear that a larger κ yields a smaller T_c and $|\Delta_d(T_c)|$. This is consistent with Eq. (11) obtained in the limit that $\kappa T \gg 1$.

It is possible that deep inside the $4e$ -SC state, the translation symmetry is further broken, so that $\langle \rho_{\mathbf{p}-\mathbf{q}} \rangle \neq 0$. By symmetry, this is when the primary PDW order develops, but the actual transition temperature for the PDW state does not coincide with the mean field T_{PDW} , and it can only set in via a Kosterlitz-Thouless transition (since a $U(1)$ translation symmetry is broken) at much lower temperature, which is beyond the scope of our GL analysis and calls for other approaches, e.g., numerics or the nonlinear sigma model in Ref. [15].

Outlook.— The d -wave symmetry for the $4e$ -SC order can be directly measured by phase-sensitive experiments, just like its $2e$ -SC counterpart [57]. Our theory has interesting implications for unconventional superconductors. There exist strong evidence for PDW in underdoped cuprates such as in LBCO near $1/8$ doping, where in-plane superconducting fluctuations, together with intertwined density-wave orders, develop at a higher temperature than the bulk superconducting temperature. [25] The PDW wave vector was proposed to be unidirectional within each Cu-O plane and alters between x and y ordering direction between neighboring planes [43], which is consistent with recent measurements in c -axis transport [58]. Our work points to a possibility of $4e$ -SC with a relative sign change between neighboring Cu-O planes with perpendicular PDW wavevectors, although microscopic details, such as whether Eq. (1) is approximately satisfied, call for a separate analysis. In addition, both PDW and $4e$ -SC (and $6e$ -SC) have been proposed to exist in the Kagome metal CsV_3Sb_5 [59–63]. It would be interesting to generalize our theory to hexagonal systems, which may be applied to CsV_3Sb_5 .

Finally, we note that our theoretical treatment of the $4e$ -SC transition, like many previous analyses of vestigial orders [18, 21, 22, 55, 56], is ultimately a mean-field

theory, which focuses on certain channels of fluctuation while neglecting others. In our work, based on analytical calculations, we specifically neglected fluctuations in the nematic, CDW, and s -wave $4e$ -SC channels. Nevertheless, it would be interesting to test our results via unbiased numerical simulations, such as quantum Monte Carlo. We leave this to future work.

ACKNOWLEDGMENTS

Acknowledgments.— The authors would like to thank Andrey Chubukov, Rafael Fernandes, Sri Raghu, Pavel Nosov, Hong Yao and Steven Kivelson for useful discussions. Y.-M. Wu acknowledges the Gordon and Betty Moore Foundation’s EPiQS Initiative through GBMF8686 for support at Stanford University. Y. Wang is supported by NSF under award number DMR-2045781. *Competing Interests.*— The Authors declare no Competing Financial or Non-Financial Interests.

Data availability.— Data will be kept in UF database and will be available upon request.

Author contributions.— Y. Wu and Y. Wang performed analytic calculations. Y. Wu performed the numerical calculations. Both authors wrote the draft.

-
- [1] G. Röpke, A. Schnell, P. Schuck, and P. Nozières, Four-particle condensate in strongly coupled fermion systems, *Phys. Rev. Lett.* **80**, 3177 (1998).
 - [2] C. Wu, Competing orders in one-dimensional spin-3/2 fermionic systems, *Phys. Rev. Lett.* **95**, 266404 (2005).
 - [3] A. A. Aligia, A. P. Kampf, and J. Mannhart, Quartet formation at (100)/(110) interfaces of d -wave superconductors, *Phys. Rev. Lett.* **94**, 247004 (2005).
 - [4] E. V. Herland, E. Babaev, and A. Sudbø, Phase transitions in a three dimensional $u(1) \times u(1)$ lattice london superconductor: Metallic superfluid and charge- $4e$ superconducting states, *Phys. Rev. B* **82**, 134511 (2010).
 - [5] B. Svistunov, E. Babaev, and N. Prokofev, *Superfluid States of Matter* (CRC Press, 2015).
 - [6] P. Li, K. Jiang, and J. Hu, Charge $4e$ superconductor: a wavefunction approach (2022), [arXiv:2209.13905 \[cond-mat.supr-con\]](https://arxiv.org/abs/2209.13905).
 - [7] J. Ge, P. Wang, Y. Xing, Q. Yin, H. Lei, Z. Wang, and J. Wang, Discovery of charge- $4e$ and charge- $6e$ superconductivity in kagome superconductor csv_3sb_5 [10.48550/ARXIV.2201.10352](https://arxiv.org/abs/2201.10352) (2022).
 - [8] N. V. Gnezdilov and Y. Wang, Solvable model for a charge- $4e$ superconductor, *Phys. Rev. B* **106**, 094508 (2022).
 - [9] Y.-F. Jiang, Z.-X. Li, S. A. Kivelson, and H. Yao, Charge- $4e$ superconductors: A majorana quantum monte carlo study, *Phys. Rev. B* **95**, 241103 (2017).
 - [10] G. Volovik, *Exotic Properties Of Superfluid Helium 3*, Series In Modern Condensed Matter Physics (World Scientific Publishing Company, 1992).
 - [11] E.-G. Moon, Skyrmions with quadratic band touching fermions: A way to achieve charge $4e$ superconductivity, *Phys. Rev. B* **85**, 245123 (2012).
 - [12] E. Fradkin, S. A. Kivelson, and J. M. Tranquada, Colloquium: Theory of intertwined orders in high temperature superconductors, *Rev. Mod. Phys.* **87**, 457 (2015).
 - [13] E. Babaev, A. Sudbø, and N. W. Ashcroft, A superconductor to superfluid phase transition in liquid metallic hydrogen, *Nature* **431**, 666 (2004).
 - [14] D. F. Agterberg and H. Tsunetsugu, Dislocations and vortices in pair-density-wave superconductors, *Nature Physics* **4**, 639 (2008).
 - [15] E. Berg, E. Fradkin, and S. A. Kivelson, Charge- $4e$ superconductivity from pair-density-wave order in certain high-temperature superconductors, *Nature Physics* **5**, 830 (2009).
 - [16] L. Radzihovsky and A. Vishwanath, Quantum liquid crystals in an imbalanced fermi gas: Fluctuations and fractional vortices in larkin-ovchinnikov states, *Phys. Rev. Lett.* **103**, 010404 (2009).
 - [17] D. F. Agterberg, M. Geracie, and H. Tsunetsugu, Conventional and charge-six superfluids from melting hexagonal fulde-ferrell-larkin-ovchinnikov phases in two dimensions, *Phys. Rev. B* **84**, 014513 (2011).
 - [18] R. M. Fernandes and L. Fu, Charge- $4e$ superconductivity from multicomponent nematic pairing: Application to twisted bilayer graphene, *Phys. Rev. Lett.* **127**, 047001 (2021).
 - [19] S.-K. Jian, Y. Huang, and H. Yao, Charge- $4e$ superconductivity from nematic superconductors in two and three dimensions, *Phys. Rev. Lett.* **127**, 227001 (2021).
 - [20] Y.-B. Liu, J. Zhou, C. Wu, and F. Yang, Charge $4e$ superconductivity and chiral metal in the 45° -twisted bilayer cuprates and similar materials (2023), [arXiv:2301.06357](https://arxiv.org/abs/2301.06357)

- [cond-mat.supr-con].
- [21] P. P. Poduval and M. S. Scheurer, [Vestigial singlet pairing in a fluctuating magnetic triplet superconductor: Applications to graphene moiré systems](#). arxiv.2301.01344 (2023).
- [22] M. Hecker, R. Willa, J. Schmalian, and R. M. Fernandes, Cascade of vestigial orders in two-component superconductors: nematic, ferromagnetic, s-wave charge-4e, and d-wave charge-4e states. arxiv:2303.00653 (2023), arXiv:2303.00653 [cond-mat.supr-con].
- [23] M. Hecker and R. M. Fernandes, Local condensation of charge-4e superconductivity at a nematic domain wall (2023), arXiv:2311.02005 [cond-mat.supr-con].
- [24] R. Liu, W. Wang, and X. Cui, Quartet superfluid in two-dimensional mass-imbalanced fermi mixtures, *Phys. Rev. Lett.* **131**, 193401 (2023).
- [25] D. F. Agterberg, J. S. Davis, S. D. Edkins, E. Fradkin, D. J. Van Harlingen, S. A. Kivelson, P. A. Lee, L. Radzihovsky, J. M. Tranquada, and Y. Wang, The physics of pair-density waves: Cuprate superconductors and beyond, *Annual Review of Condensed Matter Physics* **11**, 231 (2020).
- [26] P. Fulde and R. A. Ferrell, Superconductivity in a strong spin-exchange field, *Phys. Rev.* **135**, A550 (1964).
- [27] A. I. Larkin and Y. N. Ovchinnikov, Nonuniform state of superconductors, *Sov. Phys. JETP* **20**, 762 (1965).
- [28] C. C. Agosta, Inhomogeneous superconductivity in organic and related superconductors, *Crystals* **8**, 285 (2018).
- [29] Y. Matsuda and H. Shimahara, Fulde-ferrell-larkin-ovchinnikov state in heavy fermion superconductors, *Journal of the Physical Society of Japan* **76**, 051005 (2007).
- [30] A. Gurevich, Upper critical field and the fulde-ferrell-larkin-ovchinnikov transition in multiband superconductors, *Phys. Rev. B* **82**, 184504 (2010).
- [31] C.-w. Cho, J. H. Yang, N. F. Q. Yuan, J. Shen, T. Wolf, and R. Lortz, Thermodynamic evidence for the fulde-ferrell-larkin-ovchinnikov state in the $k\text{Fe}_2\text{As}_2$ superconductor, *Phys. Rev. Lett.* **119**, 217002 (2017).
- [32] X. Liu, Y. X. Chong, R. Sharma, and J. C. S. Davis, Discovery of a cooper-pair density wave state in a transition-metal dichalcogenide, *Science* **372**, 1447 (2021).
- [33] Y.-M. Wu, Z. Wu, and H. Yao, Pair-density-wave and chiral superconductivity in twisted bilayer transition metal dichalcogenides, *Phys. Rev. Lett.* **130**, 126001 (2023).
- [34] Z. Wu, Y.-M. Wu, and F. Wu, Pair density wave and loop current promoted by van hove singularities in moiré systems, *Phys. Rev. B* **107**, 045122 (2023).
- [35] G. Y. Cho, J. H. Bardarson, Y.-M. Lu, and J. E. Moore, Superconductivity of doped weyl semimetals: Finite-momentum pairing and electronic analog of the $^3\text{He-A}$ phase, *Phys. Rev. B* **86**, 214514 (2012).
- [36] G. Bednik, A. A. Zyuzin, and A. A. Burkov, Superconductivity in weyl metals, *Phys. Rev. B* **92**, 035153 (2015).
- [37] D. Shaffer, F. J. Burnell, and R. M. Fernandes, [Weak-coupling theory of pair density-wave instabilities in transition metal dichalcogenides](#). arxiv.2209.14469 (2022).
- [38] D. Shaffer and L. H. Santos, [Triplet pair-density wave superconductivity on the \$\pi\$ -flux square lattice](#). arxiv.2210.16324 (2022).
- [39] D. Shaffer, J. Wang, and L. H. Santos, Theory of hofstadter superconductors, *Phys. Rev. B* **104**, 184501 (2021).
- [40] E. Berg, E. Fradkin, S. A. Kivelson, and J. M. Tranquada, Striped superconductors: how spin, charge and superconducting orders intertwine in the cuprates, *New Journal of Physics* **11**, 115004 (2009).
- [41] M. Hücker, M. v. Zimmermann, G. D. Gu, Z. J. Xu, J. S. Wen, G. Xu, H. J. Kang, A. Zheludev, and J. M. Tranquada, Stripe order in superconducting $\text{La}_{2-x}\text{Ba}_x\text{CuO}_4$ ($0.095 \leq x \leq 0.155$), *Phys. Rev. B* **83**, 104506 (2011).
- [42] Y. Wang, D. F. Agterberg, and A. Chubukov, Coexistence of charge-density-wave and pair-density-wave orders in underdoped cuprates, *Phys. Rev. Lett.* **114**, 197001 (2015).
- [43] E. Berg, E. Fradkin, E.-A. Kim, S. A. Kivelson, V. Oganesyan, J. M. Tranquada, and S. C. Zhang, Dynamical layer decoupling in a stripe-ordered high- T_c superconductor, *Phys. Rev. Lett.* **99**, 127003 (2007).
- [44] Y. Wang, D. F. Agterberg, and A. Chubukov, Interplay between pair- and charge-density-wave orders in underdoped cuprates, *Phys. Rev. B* **91**, 115103 (2015).
- [45] P. A. Lee, Amperean pairing and the pseudogap phase of cuprate superconductors, *Phys. Rev. X* **4**, 031017 (2014).
- [46] L. Nie, G. Tarjus, and S. A. Kivelson, Quenched disorder and vestigial nematicity in the pseudogap regime of the cuprates, *Proceedings of the National Academy of Sciences* **111**, 7980 (2014).
- [47] C. Setty, L. Fanfarillo, and P. J. Hirschfeld, Microscopic mechanism for fluctuating pair density wave (2021), arXiv:2110.13138 [cond-mat.supr-con].
- [48] C. Setty, J. Zhao, L. Fanfarillo, E. W. Huang, P. J. Hirschfeld, P. W. Phillips, and K. Yang, Exact solution for finite center-of-mass momentum cooper pairing (2022), arXiv:2209.10568 [cond-mat.supr-con].
- [49] Y.-M. Wu, P. A. Nosov, A. A. Patel, and S. Raghu, Pair density wave order from electron repulsion, *Phys. Rev. Lett.* **130**, 026001 (2023).
- [50] K. S. Huang, Z. Han, S. A. Kivelson, and H. Yao, Pair-density-wave in the strong coupling limit of the holstein-hubbard model, *npj Quantum Materials* **7**, 17 (2022).
- [51] H.-C. Jiang, Superconductivity in the doped quantum spin liquid on the triangular lattice, *npj Quantum Materials* **6**, 71 (2021).
- [52] H. Li, H. Li, Z. Wang, S. Wan, H. Yang, and H.-H. Wen, Low-energy gap emerging from confined nematic states in extremely underdoped cuprate superconductors, *npj Quantum Materials* **8**, 18 (2023).
- [53] C. Peng, Y.-F. Jiang, T. P. Devereaux, and H.-C. Jiang, Precursor of pair-density wave in doping kitaev spin liquid on the honeycomb lattice, *npj Quantum Materials* **6**, 64 (2021).
- [54] See the supplementary material for information about i) why the models that we use are free from fine tuning, ii) how to obtain the complete expansion of the pdw fields to eighth order, iii) how the vestigial cdw order is suppressed iv) how to obtain the gl free energy for the d -wave charge-4e superconductivity and v) demonstrate the equivalence between hubbard-stratonovich transformation and the use of lagrangian multipliers.
- [55] Y. Wang and A. Chubukov, Charge-density-wave order with momentum $(2q, 0)$ and $(0, 2q)$ within the spin-fermion model: Continuous and discrete symmetry breaking, preemptive composite order, and relation to pseudogap in hole-doped cuprates, *Phys. Rev. B* **90**, 035149 (2014).
- [56] R. M. Fernandes, A. V. Chubukov, J. Knolle, I. Eremin,

- and J. Schmalian, Preemptive nematic order, pseudogap, and orbital order in the iron pnictides, *Phys. Rev. B* **85**, 024534 (2012).
- [57] C. C. Tsuei and J. R. Kirtley, Pairing symmetry in cuprate superconductors, *Rev. Mod. Phys.* **72**, 969 (2000).
- [58] Z. Shi, P. G. Baity, J. Terzic, T. Sasagawa, and D. Popović, Pair density wave at high magnetic fields in cuprates with charge and spin orders, *Nature Communications* **11**, 3323 (2020).
- [59] Y. Yu, Non-degenerate surface pair density wave in the kagome superconductor CsV_3Sb_5 – application to vestigial orders (2023), [arXiv:2210.00023](https://arxiv.org/abs/2210.00023) [cond-mat.supr-con].
- [60] Y.-M. Wu, R. Thomale, and S. Raghu, Sublattice interference promotes pair density wave order in kagome metals. [arxiv.2211.01388](https://arxiv.org/abs/2211.01388) (2022).
- [61] S. Zhou and Z. Wang, Chern fermi pocket, topological pair density wave, and charge-4e and charge-6e superconductivity in kagomé superconductors, *Nature Communications* **13**, 7288 (2022).
- [62] T. Schwemmer, H. Hohmann, M. Dürrnagel, J. Potten, J. Beyer, S. Rachel, Y.-M. Wu, S. Raghu, T. Müller, W. Hanke, and R. Thomale, Pair density wave instability in the kagome hubbard model (2023), [arXiv:2302.08517](https://arxiv.org/abs/2302.08517) [cond-mat.str-el].
- [63] H. D. Scammell, J. Ingham, T. Li, and O. P. Sushkov, Chiral excitonic order from twofold van hove singularities in kagome metals, *Nature Communications* **14**, 605 (2023).

Supplementary Material for “*d*-wave Charge-4e Superconductivity From Fluctuating Pair Density Waves”

Yi-Ming Wu¹ and Yuxuan Wang²

¹*Stanford Institute for Theoretical Physics, Stanford University, Stanford, California 94305, USA*

²*Department of Physics, University of Florida, Gainesville, Florida 32611, USA*

(Dated: August 13, 2024)

SUPPLEMENTARY NOTE I. THE FINE-TUNING-FREE MODELS

In the main text, we have made the statement that in a four-fold rotational system with four different PDW momenta, the charge-4e superconductivity channel is enhanced as long as the the PDW momentum magnitude $|\mathbf{Q}|$ and the Fermi momentum \mathbf{k}_F satisfies a specific relation

$$|\mathbf{Q}| = \sqrt{2}|\mathbf{k}_F \bmod (\pi, 0)|. \quad (\text{S1})$$

At a first glance, one might think this relation requires some fine tuning of the Fermi surfaces. However, it does not. To see this, we consider the two situations discussed in Fig. 1(c) and (d) in the main text.

In the first model, the main contribution to the PDW pairing comes from those fermions close to the Van Hove singularity points at $(\pi, 0)$ or $(0, \pi)$, since these places are where the fermion density of states maximizes. In [Supplementary Figure 1\(a\)](#) we show two typical examples of this model. The Fermi surfaces (blue curves) are obtained by a tight binding model on a square lattice with either positive or negative next nearest neighbor hopping, and the onset of PDW has been demonstrated in Ref. [1]. Reproducing the calculation there, we find that the PDW wave vectors are close to (π, π) . In [Supplementary Figure 1\(a\)](#), the heat map shows the inverse of the PDW susceptibility near the ordering vectors. We see that as long as the four-fold rotational symmetry is respected and the system is close to Van Hove filling, i.e. the four blue points near the Van Hove points form a square, then the PDW momenta (red points) automatically satisfies Eq. (S1), regardless of the filling, and hopping parameters of the model. Therefore, it is free of fine tuning.

Another example is given by the hot spot theory of superconductivity on a square lattice, which is demonstrate in [Supplementary Figure 1 \(b\)](#). Here we also choose two generic sets of parameters and obtain two configurations. In this model, the blue points, which are the intersections between the Fermi surface and the umklapp surfaces, are called hot spots. These points are the most likely positions where fermions can be scattered by the collective anti-ferromagnetic fluctuations carrying momentum (π, π) , and the pairing mechanism is driven by this collective fluctuation mediated interactions [2]. Again, as long as the four-fold rotation symmetry is respected, the four closest hot spots form a square, and the resulting PDW momentum automatically satisfies Eq. (S1). Note here both \mathbf{k}_F and \mathbf{Q} are measured from either $(\pi, 0)$ or $(0, \pi)$.

From the above discussion and [Supplementary Figure 1](#) we see that changing the electron (hole) filing fraction, or the hopping amplitude, or adding longer range hoppings, will surely change the shape of the Fermi surfaces. But as long as the four-fold rotation symmetry is present, the four active fermion spots (blue points) form a square, which is inscribed in another square formed from the resulting PDW momenta (red points). The condition in Eq. (S1) is the consequence of this simple geometric relation between the two squares, and thus is free from fine tuning.

SUPPLEMENTARY NOTE II. DETAILS OF FINDING LEADING CONTRIBUTIONS UP TO $\mathcal{O}(|\Psi|^8)$

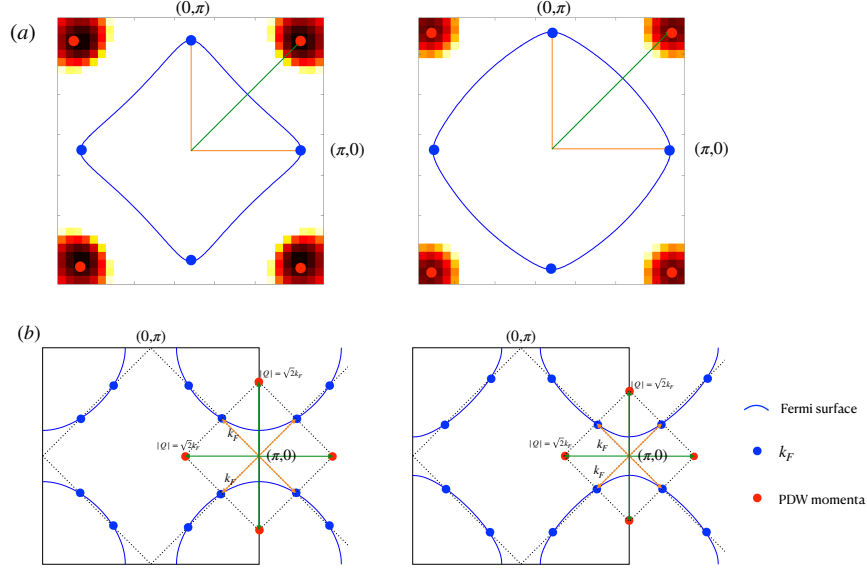
In obtaining the Ginzburg-Landau theory for the primary PDW orders, we integrate out the fermions and obtain

$$-\text{tr} \ln \mathcal{G}^{-1} \quad (\text{S2})$$

in the action. The matrix \mathcal{G} is defined as $\mathcal{G}^{-1} = G_0^{-1} + \hat{\Delta}$ and

$$G_0^{-1} = \begin{pmatrix} G_p^{-1} & 0 \\ 0 & G_h^{-1} \end{pmatrix}, \quad \hat{\Delta} = \begin{pmatrix} 0 & \Psi \\ \Psi^\dagger & 0 \end{pmatrix} \quad (\text{S3})$$

The particle and hole Green's function G_p and G_h are diagonal in frequency-momentum space. For instance, $[G_p]_{k,k'} = G_p(k)\delta_{k,k'}$. While Ψ and Ψ^\dagger is not diagonal in momentum space. In particular, we have $[\Psi]_{k,k'} = \sum_i \Psi_{\mathbf{Q}_i} \delta_{k, \mathbf{Q}_i - k'}$



Supplementary Figure 1. Illustration of the condition in Eq. (S1) for various situations in two different models. In both cases, changing electron (hole) filling, hopping amplitudes and other parameters will result in Fermi surfaces of different shapes, but the condition in Eq. (S1) can be easily satisfied without fine tuning.

and $[\Psi^\dagger]_{k,k'} = \sum_i \Psi_{\mathbf{Q}_i}^\dagger \delta_{k,-\mathbf{Q}_i-k'}$ with $\mathbf{Q}_i \in \{\pm\mathbf{Q}, \pm\mathbf{P}\}$. Expanding Eq. (S2) in terms of $\Psi_{\mathbf{Q}_i}$, we obtain

$$\begin{aligned} -\text{tr} \ln \mathcal{G}^{-1} &= -\text{tr} \ln G_0^{-1} - \text{tr} \ln(1 + G_0 \hat{\Delta}) \\ &= -\text{tr} \ln G_0^{-1} + \sum_{n=1}^{\infty} \frac{1}{2n} \text{tr}(G_0 \hat{\Delta})^{2n}. \end{aligned} \quad (\text{S4})$$

Given the matrix structure in Eq. (S3), it is easy to see that G_0 can be obtained by simply taking the inverse of the diagonal elements of G_0^{-1} . The n -th element in the series is given by

$$\begin{aligned} \frac{1}{2n} \sum_{\{k_i\}} &[G_p]_{k_1} [\Psi]_{k_1, k_2} [G_h]_{k_2} [\Psi^*]_{k_2, k_3} \dots \\ &\dots [G_p]_{k_{2n-1}} [\Psi]_{k_{2n-1}, k_{2n}} [G_h]_{k_{2n}} [\Psi^*]_{k_{2n}, k_1}, \end{aligned} \quad (\text{S5})$$

which is also shown diagrammatically in [Supplementary Figure 2](#).

In our special situation, all the Green's functions should be $G_i, i = 1, \dots, 4$, which are

$$\begin{aligned} G_1(k) &= \frac{1}{i\omega_n - v_F k_x}, G_2(k) = \frac{-1}{i\omega_n - v_F k_y}, \\ G_3(k) &= \frac{1}{i\omega_n + v_F k_x}, G_4(k) = \frac{-1}{i\omega_n + v_F k_y}. \end{aligned} \quad (\text{S6})$$

where G_1 and G_3 are particle Green's functions, while G_2 and G_4 are hole Green's functions. Given a set of Green's functions, the external momentum can be determined by momentum conservation. Therefore, each diagram uniquely corresponds to one permutation of the Green's function set. We can develop a simple algorithm to numerate all the possible combinations for any n based on Eq. (S5). The algorithm processes as follows,

1. For a given n , specify all possible set S for $2n$ Green's functions that satisfy the momentum conservation rule. For instance, for $n = 2$, one possible set is $S = \{1, 2, 3, 4\}$, meaning all the leading contributions corresponds to all the permutations of this set.
2. Generate all possible permutations for the set S , and keep only those nonequivalent ones.
3. Identify external legs for each nonequivalent permutations based on momentum conservation.

4. collect all the terms from different permutations for a given set, repeat the procedure for all sets.

It is easy to implement this algorithm to numerate all possible terms that satisfy the above conditions. For the quartic term (4-leg diagrams), we find the following contributions,

$$\beta_1 |\Psi_i|^4 + \beta_2 |\Psi_{\pm P}|^2 |\Psi_{\pm Q}|^2 + \beta (\Psi_P \Psi_{-P} \Psi_Q^* \Psi_{-Q}^* + h.c.). \quad (S7)$$

Note the last β -term is represented by the diagram shown in Fig.1(a) of the main text. The corresponding coefficients are calculated as one-loop integral of four fermion Green's functions (Eq. (S6)),

$$\begin{aligned} \beta_1 &= \frac{T}{4\pi^2 v_F^2} \sum_n \int_{-E_F}^{E_F} \frac{dx dy}{(i\omega_n - x)^2 (i\omega_n - y)^2}, \\ \beta_2 &= \frac{T}{4\pi^2 v_F^2} \sum_n \int_{-E_F}^{E_F} \frac{-dx dy}{(i\omega_n - x)^2 (\omega_n^2 + y^2)}, \\ \beta &= \frac{T}{4\pi^2 v_F^2} \sum_n \int_{-E_F}^{E_F} \frac{dx dy}{(\omega_n^2 + x^2)(\omega_n^2 + y^2)}. \end{aligned} \quad (S8)$$

If we set $k_F = E_F/v_F = 1$ and measure all the energies in units of E_F , then the above momentum integration and frequency summation can be done explicitly, leading to

$$\beta_1 \sim 1, \quad \beta_2 \sim \ln \frac{1}{T}, \quad \beta = \frac{1}{16T}. \quad (S9)$$

For the 6-leg and 8-leg diagrams, the leading contributions in terms of E_F/T at each order are

$$\begin{aligned} &\gamma \left[(|\Psi_Q|^2 + |\Psi_{-Q}|^2) |\Psi_P|^2 |\Psi_{-P}|^2 + (|\Psi_P|^2 + |\Psi_{-P}|^2) |\Psi_Q|^2 |\Psi_{-Q}|^2 + \left(\sum_{i=1}^4 |\Psi_{Q_i}|^2 \right) (\Psi_P^* \Psi_{-P}^* \Psi_Q \Psi_{-Q} + h.c.) \right] \\ &+ \frac{\zeta}{2} \left[(\Psi_P^* \Psi_{-P}^* \Psi_Q \Psi_{-Q})^2 + h.c. \right] + 4\zeta |\Psi_Q \Psi_{-Q} \Psi_P \Psi_{-P}|^2 + \zeta (|\Psi_P|^2 |\Psi_{-P}|^2 + |\Psi_Q|^2 |\Psi_{-Q}|^2) (\Psi_P^* \Psi_{-P}^* \Psi_Q \Psi_{-Q} + h.c.) \\ &+ \frac{\zeta}{4} \left(\sum_{i=1}^4 |\Psi_i|^4 \right) (\Psi_P^* \Psi_{-P}^* \Psi_Q \Psi_{-Q} + h.c.) + \frac{\zeta}{2} (|\Psi_Q|^4 + |\Psi_{-Q}|^4) |\Psi_P|^2 |\Psi_{-P}|^2 + \frac{\zeta}{2} (|\Psi_P|^4 + |\Psi_{-P}|^4) |\Psi_Q|^2 |\Psi_{-Q}|^2 \\ &+ \frac{\zeta}{2} (|\Psi_P|^2 + |\Psi_{-P}|^2) (|\Psi_Q|^2 + |\Psi_{-Q}|^2) [|\Psi_P|^2 |\Psi_{-P}|^2 + |\Psi_Q|^2 |\Psi_{-Q}|^2 + 2 (\Psi_P^* \Psi_{-P}^* \Psi_Q \Psi_{-Q} + h.c.)], \end{aligned} \quad (S10)$$

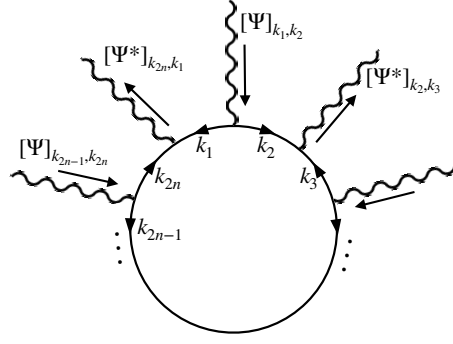
For compactness we have suppressed the momenta carried by each fields and the integration over conserved momenta.

Below we briefly discuss how to obtain (S10). For $n = 3$, the internal Green's functions runs over the set $\{1, 2, 3, 4, 1, 2\}$, where we denote G_i by i for brevity. Note that the set is equivalent to $\{1, 2, 3, 4, 2, 3\}$, $\{1, 2, 3, 4, 3, 4\}$ and $\{1, 2, 3, 4, 4, 1\}$ by D_4 symmetry. Thus all of these sets should be considered, and they combined to give the γ terms in Eq. (S10).

The results for $n = 4$ contains more terms. First of all, all the fermion Green's functions can run over the set $\{1, 2, 3, 4, 1, 2, 3, 4\}$. The set is invariant under D_4 group operation so this is a complete class. The momentum integral yields a factor of ζ for this class, and this is presented in the second line of Eq. (S10). The second class comes from the set $\{1, 2, 3, 4, 1, 1, 2, 2\}$ and its symmetry related ones $\{1, 2, 3, 4, 2, 2, 3, 3\}$, $\{1, 2, 3, 4, 3, 3, 4, 4\}$ and $\{1, 2, 3, 4, 4, 4, 1, 1\}$. The one-loop integral for these diagrams leads to a factor of $\zeta/4$, and this class corresponds to the third line of Eq. (S10). The last class comes from the set $\{1, 2, 3, 4, 1, 1, 2, 4\}$, $\{1, 2, 3, 4, 2, 2, 1, 3\}$, $\{1, 2, 3, 4, 3, 3, 2, 4\}$ and $\{1, 2, 3, 4, 4, 4, 1, 3\}$, for which the one-loop integral yields a factor of $\zeta/2$. This corresponds to the last line of Eq. (S10). It can be checked that all other sets doest not meet the momentum conservation, i.e. they will lead to some external legs for which the momentum is neither $\pm Q$ nor $\pm P$. Therefore, Eq. (S10) is all the leading contributions at $\mathcal{O}(|\Psi_{Q_i}|^8)$.

Similarly, the coefficients of γ and ζ are given by one-loop integration of six and eight Green's functions, namely

$$\begin{aligned} \gamma &= T \sum_n \int \frac{dx dy}{4\pi^2} \left(\frac{1}{i\omega_n - x} \right)^2 \left(\frac{1}{i\omega_n - y} \right)^2 \frac{1}{i\omega_n + x} \frac{-1}{i\omega_n + y} \\ &= \frac{1}{16T^3 \pi^4} \sum_{n=-\infty}^{+\infty} \frac{1}{(2n+1)^4} \\ &= \frac{1}{768T^3}, \end{aligned} \quad (S11)$$



Supplementary Figure 2. A general diagrammatic representation for higher-order interactions of PDW bosons.

and

$$\begin{aligned}
\zeta &= T \sum_n \frac{dx dy}{4\pi^2} \left(\frac{1}{i\omega_n - x} \right)^2 \left(\frac{1}{i\omega_n - y} \right)^2 \left(\frac{1}{i\omega_n + x} \right)^2 \left(\frac{1}{i\omega_n + y} \right)^2 \\
&= \frac{1}{16T^5 \pi^6} \sum_{n=-\infty}^{+\infty} \frac{1}{(2n+1)^6} \\
&= \frac{1}{7680T^5}.
\end{aligned} \tag{S12}$$

SUPPLEMENTARY NOTE III. DETAILS ON DECOUPLING THE PDW FIELDS

The higher-order interactions presented in Eq. (S10) can be greatly simplified by using composite fields including those corresponding to 4e-SC

$$\begin{aligned}
\Psi_P^* \Psi_{-P}^* \Psi_Q \Psi_{-Q} + h.c. &= \frac{1}{2} |\Phi_s|^2 - \frac{1}{2} |\Phi_d|^2, \\
|\Psi_P|^2 |\Psi_{-P}|^2 &= \frac{1}{4} |\Phi_s - \Phi_d|^2, \\
|\Psi_Q|^2 |\Psi_{-Q}|^2 &= \frac{1}{4} |\Phi_s + \Phi_d|^2, \\
\Psi_Q \Psi_{-Q} \Psi_P \Psi_{-P} &= \frac{1}{16} (\Phi_s^2 - \Phi_d^2) \\
(|\Psi_P|^2 + |\Psi_{-P}|^2) (|\Psi_Q|^2 + |\Psi_{-Q}|^2) &= \frac{1}{4} (\phi^2 - \mathcal{N}^2),
\end{aligned} \tag{S13}$$

where in the last line $\phi \equiv |\Psi_P|^2 + |\Psi_{-P}|^2 + |\Psi_Q|^2 + |\Psi_{-Q}|^2$ is the Gaussian fluctuation and $\mathcal{N} \equiv |\Psi_P|^2 + |\Psi_{-P}|^2 - |\Psi_Q|^2 - |\Psi_{-Q}|^2$ is the nematic order. It is important to note that this re-expression of quartic combinations of Ψ in terms of bilinear operators is not unique. For example, $|\Psi_P|^2 |\Psi_{-P}|^2$ can also be rewritten as $[(|\Psi_P|^2 + |\Psi_{-P}|^2)^2 - (|\Psi_P|^2 - |\Psi_{-P}|^2)^2]/4$, which does not explicitly depend on 4e-SC fluctuations. However, the re-expression can be made unique after extending the Ψ field to an M -component Ψ^I , e.g.,

$$|\Psi_P|^2 |\Psi_{-P}|^2 \rightarrow \frac{1}{M} \sum_{I,J=1}^M \Psi_P^I \Psi_P^{*J} \Psi_{-P}^I \Psi_{-P}^{*J} \equiv \frac{M}{4} |\Phi_s - \Phi_d|^2. \tag{S14}$$

$$\text{where } \Phi_{s,d} = \frac{1}{M} \sum_I (\Psi_Q^I \Psi_{-Q}^I \pm \Psi_P^I \Psi_{-P}^I). \tag{S15}$$

Such a large- M extension justifies the mean-field theory for 4e-SC, and thus different extension schemes correspond to different mean-field ansätze.

We insert to the partition function the following δ -function identities [3]

$$\begin{aligned} 1 &\propto \int \mathcal{D}[\lambda_d, \Delta_d^*] \exp \left[-\frac{1}{T} \int_{\mathbf{q}} \lambda_d(\mathbf{q}) (\Delta_d^*(-\mathbf{q}) - \Phi_d^*(\mathbf{q})) \right] \\ 1 &\propto \int \mathcal{D}[\varphi, \mu] \exp \left[-\frac{1}{T} \int_{\mathbf{q}} \mu(\mathbf{q}) (\varphi(-\mathbf{q}) - \phi(-\mathbf{q})) \right] \end{aligned} \quad (\text{S16})$$

and the saddle points for the λ 's and μ ensures that one can replace in Eq. (S10) the bilinear fluctuations Φ_d and ϕ with local fields Δ_d and φ . The resulting theory is

$$\begin{aligned} F[\Psi, \Delta_d, \varphi, \lambda_d, \mu] &= \sum_i \int_{\mathbf{q}} [\alpha(T) + \kappa \mathbf{q}^2] |\Psi_i(\mathbf{q})|^2 - \frac{\beta}{2} \int_{\mathbf{q}} |\Delta_d(\mathbf{q})|^2 - \frac{\gamma}{4} \int_{\mathbf{q}, \mathbf{p}} \Delta_d(\mathbf{q}) \Delta_d^*(\mathbf{q} + \mathbf{p}) \phi(\mathbf{p}) \\ &+ \frac{\zeta}{16} \int_{\mathbf{q}, \mathbf{k}, \mathbf{p}} \Delta_d(\mathbf{q}) \Delta_d^*(\mathbf{q} + \mathbf{p}) \Delta_d(\mathbf{k}) \Delta_d^*(\mathbf{k} - \mathbf{p}) - \frac{\zeta}{16} \int_{\mathbf{q}, \mathbf{k}, \mathbf{p}} \Delta_d(\mathbf{q}) \Delta_d^*(\mathbf{q} + \mathbf{p}) \varphi(\mathbf{k}) \varphi(\mathbf{p} - \mathbf{k}) \\ &+ \int_{\mathbf{q}} [\lambda_d(\mathbf{q}) (\Delta_d^*(\mathbf{q}) - \Phi_d^*(\mathbf{q})) + h.c.] + \int_{\mathbf{q}} \mu(\mathbf{q}) (\varphi(-\mathbf{q}) - \phi(-\mathbf{q})) + \mathcal{O}(\Psi^{10}) \end{aligned} \quad (\text{S17})$$

As a mean-field ansatz, we consider saddle-point solutions of the composite fields that are spatially uniform, with $\Delta_d(\mathbf{q}) = \Delta_d \delta(\mathbf{q})$, and $\varphi(\mathbf{q}) = \varphi \delta(\mathbf{q})$. Using the regularization $\delta(\mathbf{q} = 0) = V$ where V is the volume (area) of the system and defining the free energy density $\mathcal{F} \equiv F/V$, Eq. (S17) then becomes

$$\begin{aligned} \mathcal{F}[\Psi, \Delta_d, \varphi, \lambda_d, \mu] &= \sum_{i, \mathbf{q}} \left[\alpha(T) + \kappa \mathbf{q}^2 - \frac{\gamma}{4} |\Delta_d|^2 - \mu \right] |\Psi_i(\mathbf{q})|^2 - \frac{\beta}{2} |\Delta_d|^2 + \frac{\zeta}{16} |\Delta_d|^4 - \frac{\zeta}{16} |\Delta_d|^2 \varphi^2 \\ &+ \lambda_d (\Delta_d^* - \Phi_d^*) + \lambda_d^* (\Delta_d - \Phi_d) + \mu \varphi + \mathcal{O}(\Psi^{10}), \end{aligned} \quad (\text{S18})$$

where $\lambda_d \equiv \lambda_d(\mathbf{q} = 0)/V$, $\mu \equiv \mu(\mathbf{q} = 0)/V$, and we have used the fact that $V \int_{\mathbf{q}} \equiv \sum_{\mathbf{q}}$ in the continuum limit.

SUPPLEMENTARY NOTE IV. DETAILS ON MEAN-FIELD THEORY FOR $4e$ -SC

To justify a mean-field theory, we formally extend Eq. (S18) to a large- M version using the scheme described in Eq. (S15). Together with rescaling $\lambda_d \rightarrow M\lambda_d$ and $\mu \rightarrow M\mu$, Eq. (S18) becomes

$$\begin{aligned} \mathcal{F}[\Psi, \Delta_d, \varphi, \lambda_d, \mu] &= \sum_{J=1}^M \sum_i \int_{\mathbf{q}} \left[\alpha(T) + \kappa \mathbf{q}^2 - \frac{\gamma}{4} |\Delta_d|^2 - \mu \right] |\Psi_i^J(\mathbf{q})|^2 - \frac{M\beta}{2} |\Delta_d|^2 + \frac{M\zeta}{16} |\Delta_d|^4 - \frac{M\zeta}{16} |\Delta_d|^2 \varphi^2 \\ &+ M\lambda_d (\Delta_d^* - \Phi_d^*) + M\lambda_d^* (\Delta_d - \Phi_d) + M\mu \varphi + \mathcal{O}(\Psi^{10}). \end{aligned} \quad (\text{S19})$$

Since \mathcal{F} is quadratic in Ψ , we can integrate it out. We get, up to higher-order terms

$$\begin{aligned} \mathcal{F}(\Delta_d, \varphi, \lambda_d, \mu)/M &= 2T \int_{\mathbf{q}} \ln \left[(\alpha(T) + \kappa \mathbf{q}^2 - \frac{\gamma}{4} |\Delta_d|^2 - \mu)^2 - |\lambda_d|^2 \right] \\ &- \frac{\beta}{2} |\Delta_d|^2 + \frac{\zeta}{16} |\Delta_d|^4 - \frac{\zeta}{16} |\Delta_d|^2 \varphi^2 + \lambda_d \Delta_d^* + \lambda_d^* \Delta_d + \mu \varphi, \end{aligned} \quad (\text{S20})$$

where the upper cutoff is a proper combination of high-energy scale E_F and short distance scale $n^{-1/2}$, which in our units is 1. We have also used $\frac{1}{V} \sum_{\mathbf{q}} \equiv \int_{\mathbf{q}}$.

In the $M \rightarrow \infty$ limit, the partition function $Z = e^{-\mathcal{F}V/T}$ is completely determined by the saddle points of $\Delta_d, \varphi, \lambda_d$ and μ . One can take the saddle-point equations to eliminate the Lagrange multiplier fields λ_d and μ . We get from

the requirements $\partial\mathcal{F}/\partial\varphi = 0$, $\partial\mathcal{F}/\partial\lambda_d^* = 0$ and $\partial\mathcal{F}/\partial\mu = 0$ that

$$\mu = \frac{\zeta}{8} |\Delta_d|^2 \varphi \quad (\text{S21})$$

$$|\lambda_d| = r \tanh \frac{2\pi\kappa|\Delta_d|}{T} \quad (\text{S22})$$

$$\varphi = \frac{T}{\pi\kappa} \ln \left(\frac{\kappa}{r} \cosh \frac{2\pi\kappa|\Delta_d|}{T} \right), \quad (\text{S23})$$

$$\text{where } r \equiv \alpha(T) - \frac{\gamma}{4} |\Delta_d|^2 - \frac{\zeta}{8} |\Delta_d|^2 \varphi, \quad (\text{S24})$$

where to obtain Eq. (S23) we have used Eq. (S22). Note that in order to legitimize the procedure of integrating out PDW orders, we need to keep r as positive definite. This will be justified in our following calculation for Δ_d . Eqs. (S21, S22) can be used to eliminate the Lagrange multiplier fields λ and μ in Eq. (S20), which yields

$$\begin{aligned} \frac{\mathcal{F}(\Delta_d)}{M} &= -\frac{\beta}{2} |\Delta_d|^2 + \frac{\zeta}{16} |\Delta_d|^4 + \frac{\zeta}{16} |\Delta_d|^2 \varphi^2 + r\varphi + \frac{rT}{\pi\kappa} \\ &= \alpha(T)\varphi - \left(\frac{\beta}{2} + \frac{T\gamma}{4\pi\kappa} \right) |\Delta_d|^2 - \left(\frac{\gamma}{4} + \frac{T\zeta}{8\pi\kappa} \right) |\Delta_d|^2 \varphi - \frac{\zeta}{16} |\Delta_d|^2 \varphi^2 + \frac{\zeta}{16} |\Delta_d|^4 + \text{const}, \end{aligned} \quad (\text{S25})$$

where at the second equality we have used Eq. (S24) to eliminate r .

The φ dependence in Eq. (S25) can be further eliminated using Eq. (S23), which does not admit a closed-form solution but can be expressed in Taylor expansion

$$\varphi = \frac{T}{\pi\kappa} \ln \frac{\kappa}{\alpha} + c_2 |\Delta_d|^2 + c_4 |\Delta_d|^4 + c_6 |\Delta_d|^6 + \dots \quad (\text{S26})$$

where the first term is the familiar logarithmic divergence of Gaussian fluctuations in 2d, and the rest is the back action from $4e$ -SC fluctuations. Substituting this expansion into Eq. (S23) and matching the coefficients on both sides, we find, omitting high-order terms in c_6 due to space,

$$\begin{aligned} c_2 &= \frac{2\pi\kappa}{T} + \frac{\gamma T}{4\pi\alpha\kappa} + \frac{\zeta T^2}{8\pi^2\alpha\kappa^2} \ln \frac{\kappa}{\alpha}, \\ c_4 &= -\frac{4\pi^3\kappa^3}{3T^3} + \frac{\zeta}{4\alpha} + \frac{\gamma^2 T}{32\pi\alpha^2\kappa} + \frac{\gamma\zeta T^2}{32\pi^2\alpha^2\kappa^2} \ln \frac{\kappa}{\alpha} + \frac{\zeta^2 T^3}{64\pi^3\alpha^2\kappa^3} \ln \frac{\kappa}{\alpha} + \frac{\zeta^2 T^3}{128\pi^3\alpha^2\kappa^3} \ln^2 \frac{\kappa}{\alpha} \\ c_6 &= \frac{64\pi^5\kappa^5}{45T^5} - \frac{\pi^2\zeta\kappa^2}{6\alpha T^2} + \dots \end{aligned} \quad (\text{S27})$$

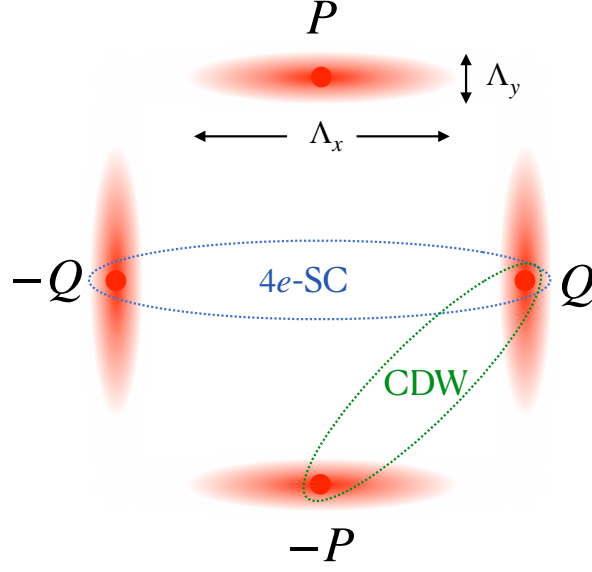
Next we integrate out the PDW fields, and replace φ , λ_d and μ with their saddle point values. This leads to the following GL free energy for Δ_d only,

$$\mathcal{F}(\Delta_d)/M = A(T)|\Delta_d|^2 + B(T)|\Delta_d|^4 + C(T)|\Delta_d|^6 + \dots, \quad (\text{S28})$$

where the GL coefficients are

$$\begin{aligned} A(T) &= \frac{2\pi\alpha\kappa}{T} - \frac{\beta}{2} - \frac{\gamma T}{4\pi\kappa} \ln \frac{\kappa}{\alpha} - \frac{\zeta T^2}{16\pi^2\kappa^2} \ln^2 \frac{\kappa}{\alpha}, \\ B(T) &= -\frac{4\pi^3\alpha\kappa^3}{3T^3} - \frac{\pi\gamma\kappa}{2T} + \frac{\zeta}{16} - \frac{\gamma^2 T}{32\pi\alpha\kappa} - \frac{\zeta}{4} \left(\frac{\gamma T^2}{8\pi^2\alpha\kappa^2} + 1 \right) \ln \frac{\kappa}{\alpha} - \frac{\zeta^2 T^3}{128\pi^3\alpha\kappa^3} \ln^2 \frac{\kappa}{\alpha}, \\ C(T) &= \frac{64\pi^5\alpha\kappa^5}{45T^5} + \frac{\pi^3\gamma\kappa^3}{3T^3} + \frac{\pi^2\zeta\kappa^2}{6T^2} \left(\ln \frac{\kappa}{\alpha} - \frac{3}{2} \right) + \dots \end{aligned} \quad (\text{S29})$$

Using Eqs. (S9, S11, and S12), we see that all terms in Eq. (S29) are actually organized in increasing powers of $1/\kappa T \ll 1$ or $1/\kappa\alpha$. Assuming $\kappa\alpha \gtrsim 1$ as we will justify below, the coefficients can be greatly simplified. Indeed, we have already omitted many terms in higher powers of $1/\kappa T$ in $C(T)$. More importantly, higher-order terms in the PDW field Ψ in Eq. (S18) in fact enter all coefficients A , B , and C , but it is straightforward to see from the pattern that they are further suppressed by $1/\kappa T$, which thereby serves as a control parameter for the perturbative expansion of the free energy in terms of the PDW fields Ψ . In the opposite limit $\kappa T \ll 1$, the effective theory for PDW bosons becomes strongly coupled, and a perturbative expansion in Ψ becomes inadequate. Keeping only the leading order contributions in the limit of $1/\kappa T, 1/\kappa\alpha \ll 1$, we arrive at Eq.(12) in the main text. In this limit, the leading contribution to $\mathcal{F}(\Delta_d)$ comes from quadratic and quartic terms of the PDW free energy.



Supplementary Figure 3. CDW order is suppressed by non-perfect nesting. In practice, the momentum integration for CDW is restricted to only a tiny area to retain the CDW momentum, which shrinks the available phase space and hence reduces the outcomes after integration.

SUPPLEMENTARY NOTE V. ANISOTROPY OF PDW STIFFNESS AND SUPPRESSION OF VESTIGIAL CDW ORDER

From Eq. (S9) we see that at low temperatures, we only need to keep the β term, which is much larger than β_1 and β_2 . But even with only this term, there are different ways of decomposing it which result in different vestigial orders. As we have discussed in the main text that the charge- $4e$ channel is the leading channel, while the CDW channel can be neglected. This is true when the primary PDW susceptibility has some anisotropy as shown in [Supplementary Figure 3](#), which is in general the case with C_4 symmetry (See also Fig.1 in our main text). For systems with continuous rotation symmetry, the anisotropy at any given PDW ordering momentum is even stronger – in one direction the inverse susceptibility is quadratic in momentum, while it is quartic in the perpendicular direction.

As can be seen in [Supplementary Figure 3](#), the red regions indicates the momentum range of soft (low-energy) PDW fluctuations, which are anisotropic around each PDW order momenta. The $4e$ -SC involves low-energy PDW bosons with opposite momenta, such that as long as one of the boson is low-energy, so does the other. However, the CDW order involves bosons that differ in momentum by, say $\mathbf{P} + \mathbf{Q}$. In order for both bosons to be low-energy, the momentum of one PDW boson should be near $\pm\mathbf{Q}$ and the other near $\mp\mathbf{P}$. Compared with that for $4e$ -SC, the effective momentum range for bosons contributing to the CDW instability is much smaller, thus leading to a much weaker tendency toward CDW. As we mentioned in the main text, this is similar to the argument in fermionic systems, in which CDW instabilities are weaker due to the general lack of nesting of the fermionic dispersion. [4].

By analyzing their free energy separately, we can show quantitatively that the $4e$ -SC order always has a higher transition temperature than CDW. We note that the same four-boson interaction can be decomposed in either the particle-particle channel or the particle-hole channel, i.e,

$$4e\text{-SC channel: } \beta \int_{\mathbf{q}_1, \mathbf{q}_2, \mathbf{q}_3} [\Psi_{\mathbf{P}}(\mathbf{q}_1) \Psi_{-\mathbf{P}}(-\mathbf{q}_1 + \mathbf{q}_3)] [\Psi_{\mathbf{Q}}^*(\mathbf{q}_2) \Psi_{-\mathbf{Q}}^*(-\mathbf{q}_2 + \mathbf{q}_3)] + h.c.. \quad (\text{S30})$$

$$\text{CDW channel: } \beta \int_{\mathbf{q}_1, \mathbf{q}_2, \mathbf{q}_3} [\Psi_{\mathbf{P}}(\mathbf{q}_1) \Psi_{\mathbf{Q}}^*(\mathbf{q}_1 + \mathbf{q}_3)] [\Psi_{-\mathbf{P}}(\mathbf{q}_2) \Psi_{-\mathbf{Q}}^*(\mathbf{q}_2 - \mathbf{q}_3)] + h.c.. \quad (\text{S31})$$

Moreover, the interaction can be made equally attractive in $4e$ -SC and CDW channels by choosing the proper sign-changing patterns in momentum space.

Due to the attractive interaction, one can separately introduce CDW and $4e$ -SC order parameters that couple to PDW bosons via the bilinear term. Separately introducing the corresponding auxiliary fields to obtain the free energies for CDW and $4e$ -SC, extending them to large- M , and integrating out the PDW field while keeping the anisotropy of

stiffness around each PDW wave vector, we have for 4e-SC order Δ_d ,

$$\begin{aligned} & \mathcal{F}_{4e}(\Delta_d, \varphi, \lambda_d, \mu)/M \\ &= 2T \int_{\mathbf{q}} \ln \det \begin{pmatrix} \kappa_1 q_x^2 + \kappa_2 q_y^2 + r(\Delta_d, \mu) & 0 & -\lambda_d & 0 \\ 0 & \kappa_1 q_y^2 + \kappa_2 q_x^2 + r(\Delta_d, \mu) & 0 & \lambda_d \\ -\bar{\lambda}_d & 0 & \kappa_1 q_x^2 + \kappa_2 q_y^2 + r(\Delta_d, \mu) & 0 \\ 0 & \bar{\lambda}_d & 0 & \kappa_1 q_y^2 + \kappa_2 q_x^2 + r(\Delta_d, \mu) \end{pmatrix} \\ & - \frac{\beta}{2} |\Delta_d|^2 + \frac{\zeta}{16} |\Delta_d|^4 - \frac{\zeta}{16} |\Delta_d|^2 \varphi^2 + \lambda_d \Delta_d^* + \lambda_d^* \Delta_d + \mu \varphi + \dots, \end{aligned} \quad (\text{S32})$$

while for CDW order Υ_d

$$\begin{aligned} & \mathcal{F}_{\text{CDW}}(\Upsilon_d, \varphi, \lambda_d, \mu)/M \\ &= 2T \int_{\mathbf{q}} \ln \det \begin{pmatrix} \kappa_1 q_x^2 + \kappa_2 q_y^2 + r(\Upsilon_d, \mu) & \lambda_d & 0 & 0 \\ \lambda_d & \kappa_1 q_y^2 + \kappa_2 q_x^2 + r(\Upsilon_d, \mu) & 0 & 0 \\ 0 & 0 & \kappa_1 q_x^2 + \kappa_2 q_y^2 + r(\Upsilon_d, \mu) & -\lambda_d \\ 0 & 0 & -\lambda_d & \kappa_1 q_y^2 + \kappa_2 q_x^2 + r(\Upsilon_d, \mu) \end{pmatrix} \\ & - \frac{\beta}{2} |\Upsilon_d|^2 + \frac{\zeta}{16} |\Upsilon_d|^4 - \frac{\zeta}{16} |\Upsilon_d|^2 \varphi^2 + \lambda_d \Upsilon_d^* + \lambda_d^* \Upsilon_d + \mu \varphi + \dots. \end{aligned} \quad (\text{S33})$$

Here in general $\kappa_1 \neq \kappa_2$, as can be seen from [Supplementary Figure 3](#), and $r(\Delta, \mu) = \alpha(T) - \frac{\gamma}{4} |\Delta|^2 - \mu$. Note that only difference between \mathcal{F}_{CDW} and \mathcal{F}_{4e} is in the off-diagonal matrix elements.

By evaluating the determinants of the 4×4 matrices, it is straightforward to see that for \mathcal{F}_{4e} , the anisotropy in $\kappa_{1,2}$ can be absorbed into a redefinition of q_x and q_y , leading to an effective $\kappa_{\text{eff}} = \sqrt{\kappa_1 \kappa_2}$ in place of the κ used in the main text and in the previous sections.

However, the same cannot be done for \mathcal{F}_{CDW} , due to the mismatch of the diagonal terms in the 2×2 blocks of the matrix. Due to this mismatch, evaluating the two determinants and using simple algebraic relations, we can prove that for the same arguments with $\lambda_d \neq 0$

$$\mathcal{F}_{\text{CDW}}(\Delta, \varphi, \lambda_d, \mu) > \mathcal{F}_{4e}(\Delta, \varphi, \lambda_d, \mu). \quad (\text{S34})$$

From Eq. (S21-S23), both free energy functions admit a trivial solution $\Delta_d = \Upsilon_d = 0$, $\lambda_d = 0$, $\mu = 0$, $\varphi = (T/\pi\kappa_{\text{eff}}) \ln \kappa/\alpha$. At these values $\mathcal{F}_{4e} = \mathcal{F}_{\text{CDW}}$, which we define as \mathcal{F}_0 . The first order phase transition occurs for 4e-SC when at a nonzero saddle-point value of Δ_{4e} , $\mathcal{F}_{4e}(\Delta_d, \varphi, \lambda_d, \mu) = \mathcal{F}_0$, such that the trivial solution is no longer the global minimum. From Eq. (S34), the saddle point value of $\mathcal{F}_{\text{CDW}}(\Upsilon_d, \varphi, \lambda_d, \mu)$ should be larger than \mathcal{F}_0 , thus indicating the CDW transition has not yet occurred. This completes our proof that 4e-SC has a higher transition temperature than the vestigial CDW order.

SUPPLEMENTARY NOTE VI. EQUIVALENCE BETWEEN HS TRANSFORMATION AND THE METHOD OF LAGRANGIAN MULTIPLIERS

In a special case when γ and ζ terms are absent from the action, one can alternatively perform HS (HS) transformation to analyze the charge-4e order. Below we show that the HS transformation yields exactly the same results as we obtain by using Lagrangian multiplier. The action we consider is

$$\int \frac{d^2 q}{4\pi^2} \left[(\kappa q^2 + \alpha) \sum_{i=1}^4 |\Psi_{\mathbf{Q}_i}|^2 \right] - \frac{\beta}{2} |\Phi_d|^2 \quad (\text{S35})$$

with $\beta > 0$. After HS transformation, the action becomes

$$\frac{\beta}{2} (|\Delta_d|^2 - \Delta_d \Phi_d^* - \bar{\Delta}_d \Phi_d) + \int \frac{d^2 q}{4\pi^2} \left[(\kappa q^2 + \alpha) \sum_{i=1}^4 |\Psi_{\mathbf{Q}_i}|^2 \right] \quad (\text{S36})$$

Again one can integrate out the PDW order parameters using the basis $\Psi = (\Psi_{\mathbf{Q}}, \Psi_{\mathbf{P}}, \Psi_{-\mathbf{Q}}^\dagger, \Psi_{-\mathbf{P}}^\dagger)^T$. This leads to the following effective action for the charge-4e order

$$\frac{\beta}{2} \Delta_d^2 + T \int \frac{d^2 q}{4\pi^2} \text{tr} \ln A(q) \quad (\text{S37})$$

where

$$A(q) = \begin{pmatrix} \kappa q^2 + \alpha & 0 & -\frac{\beta}{2}\Delta_d & 0 \\ 0 & \kappa q^2 + \alpha & 0 & \frac{\beta}{2}\Delta_d \\ -\frac{\beta}{2}\bar{\Delta}_d & 0 & \kappa q^2 + \alpha & 0 \\ 0 & \frac{\beta}{2}\bar{\Delta}_d & 0 & \kappa q^2 + \alpha \end{pmatrix}. \quad (\text{S38})$$

Performing the $\text{tr} \ln$ operation, Eq. (S2) becomes

$$\frac{\beta}{2}\Delta_d^2 + T \int \frac{d^2q}{2\pi^2} \ln \left[(\kappa q^2 + \alpha)^2 - \frac{\beta^2}{4}\Delta_d^2 \right] \quad (\text{S39})$$

The saddle point of this action reads

$$\begin{aligned} 1 &= \beta T \int \frac{d^2q}{4\pi^2} \frac{1}{(\kappa q^2 + \alpha)^2 - \frac{\beta^2}{4}\Delta_d^2} \\ &= \frac{\beta T}{4\pi\kappa} \frac{1}{\frac{\beta}{2}\Delta_d} \text{arccoth} \frac{\alpha}{\frac{\beta}{2}\Delta_d}, \end{aligned} \quad (\text{S40})$$

or equivalently,

$$\Delta_d = \frac{T}{2\pi\kappa} \text{arccoth} \frac{2\alpha}{\beta\Delta_d} \quad \text{or} \quad \tanh(2\pi\kappa\Delta_d/T) = \frac{\beta\Delta_d}{2\alpha}. \quad (\text{S41})$$

In obtaining the above saddle point equations, we have used the condition that $\alpha > \frac{\beta}{2}\Delta_d$, as is required for the convergence of the Gaussian integral in order to integrate out PDW fields. Eq. (S41) is the results obtained via HS transformation at quartic level.

To compare Eq. (S41) with the one obtained using the method of Lagrangian multiplier, we note that in the absence of γ and ζ , we have [see Eq. (S23)]

$$\varphi = \frac{T}{\pi\kappa} \ln \left(\frac{\kappa}{\alpha} \cosh \frac{2\pi\kappa|\Delta_d|}{T} \right). \quad (\text{S42})$$

The free energy for Δ_d then becomes

$$\mathcal{F}[\Delta_d] = -\frac{\beta}{2}|\Delta_d|^2 + \frac{\alpha T}{\pi\kappa} \left[1 + \ln \left(\frac{\kappa}{\alpha} \cosh \frac{2\pi\kappa|\Delta_d|}{T} \right) \right]. \quad (\text{S43})$$

Variation of this free energy with respect to $|\Delta_d|$ and set it to zero, we immediately obtain the gap equation

$$-\frac{\beta}{2}\Delta_d + \alpha \tanh(2\pi\kappa\Delta_d/T) = 0 \quad (\text{S44})$$

which is exactly the same as Eq. (S41). Therefore, we have proved that at the level of $\mathcal{O}(\Psi^4)$, both the HS transformation and the method of Lagrangian multiplier yield the same result. However, the HS transformation, which is built on Gaussian integral, fails to work once higher order terms of the primary order parameters are included, but the Lagrangian multiplier method is still valid.

- [1] Y.-M. Wu, P. A. Nosov, A. A. Patel, and S. Raghu, Pair density wave order from electron repulsion, *Phys. Rev. Lett.* **130**, 026001 (2023).
- [2] Y. Wang, D. F. Agterberg, and A. Chubukov, Coexistence of charge-density-wave and pair-density-wave orders in underdoped cuprates, *Phys. Rev. Lett.* **114**, 197001 (2015).
- [3] λ_d and λ_d^* , as well as Δ_d and Δ_d^* , are independent fields. The integration domains for λ_d , λ_d^* , and μ are along the imaginary axis, but their saddle points may not be.
- [4] Y. Wang and A. Chubukov, Charge-density-wave order with momentum $(2q, 0)$ and $(0, 2q)$ within the spin-fermion model: Continuous and discrete symmetry breaking, preemptive composite order, and relation to pseudogap in hole-doped cuprates, *Phys. Rev. B* **90**, 035149 (2014).